inter.noise 2014
MELBOURNE AUSTRALIA
16-19 NOVEMBER

Three-dimensional beamforming of aeroacoustic sources.

Ric PORTEOUS[1]; Zebb PRIME[1]; Vincent VALEAU[2]; Con DOOLAN[1]; Danielle MOREAU[1];

[1] University of Adelaide, Australia
[2] CNRS - Université de Poitiers-ENSMA, France

ABSTRACT

This paper outlines the development and implementation of an alternative beamforming processing technique known as 'multiplicative beamforming'. The technique is well suited to non-planar microphone arrays scanning a three-dimensional (3D) grid. Numerical simulations show that the technique improves 3D spatial localisation by reducing side lobe levels and removing the directional bias of the main lobe of the beamforming output. It can also be used to accurately localise dipole sound sources, which are commonly found in aeroacoustics. The technique has also been applied to experimentally obtained data measured using a non-planar array inside an open-jet anechoic wind tunnel at the University of Adelaide. The experimentally obtained results show good agreement to that of the numerically simulated results.

Keywords: Aeroacoustics, Three-dimensional Beamforming

1. INTRODUCTION

Phased microphone arrays (beamformers) are a popular method for acoustic source localisation because they can be used without mechanical movement (Brooks and Humphreys 1999). Each microphone in the array simultaneously records a noise sample and the records are delayed and summed coherently (or adjusted in the frequency domain) to enhance the signal from a focal position and minimise the signal from an out-of-focus location (Liu et al. 2008). The beamformer response is near maximum when the focal position coincides with the exact location of the source, therefore, the source location can be determined by scanning over a grid of focal points (the scanning grid), and finding the location of the maximum output. In theory, the scanning grid can be either a two-dimensional (2D) planar grid, or a three-dimensional (3D) grid consisting of several parallel planes.

Traditionally the microphones in the array are arranged in the same spatial plane (Brooks and Humphreys 2003; Prime and Doolan 2013; Geyer et al. 2012; Sarradj 2012). These are known as 'planar' arrays and these have good spatial resolution in a plane parallel to the microphones. However, they have poor spatial resolution in the direction normal to the array (Sarradj 2012). This makes it difficult to unambiguously locate sources in a 3D scanning grid.

Padois et al. (2013) have shown that non-planar arrays can improve the depth resolution of the beamformer. In their study, Padois et al. (2013) used an array containing 192 microphones positioned so that they fully enclosed the source region in four spiral patterns. The beamformer was successfully able to locate an acoustic source to within 3 cm in a potential scanning volume of of 2 m^3.

In practice, fully enclosing the source with microphones may not be feasible due to spatial limitations of the facility or due to limitations on the number of microphones. In this paper it is shown that accurate 3D source localisation can also be obtained using only two orthogonal arrays arranged so that the microphones only partially enclose the source region. Such a microphone arrangement does introduce a directional bias in the beamforming output if conventional beamforming post-processing is used. In this paper a technique known as 'multiplicative beamforming' is used as an alternative post-processing step to eliminate this directional bias. The technique also reduces side lobe levels from the beamforming map and thus improves the 3D-localisation accuracy of the microphone array.

The paper is presented as follows; first both conventional beamforming and multiplicative beamfoming post-processing techniques are discussed in Section 2. Next, the beamforming outputs of a numerically simulated source is given in Section 3 to illustrate the theoretical benefits of multiplicative beamforming. Finally, in Section 4 the method is applied to experimentally obtained data of a dipole source in an open-jet

[1] ric.porteous@adelaide.edu.au
[3] vincent.valeau@univ-poitiers.fr

wind tunnel.

2. BEAMFORMING THEORY

2.1 Conventional Beamforming

To localise an acoustic source, the beamformer is electronically 'steered' to a location in three-dimensional space, denoted $\mathbf{x_t} = (x_t, y_t, z_t)$. The output of the beamformer, $B(\mathbf{x_t}, \omega)$ is given in Equation 1, where $\mathbf{P}(\omega) = [p_1, ..., p_M]^T$ is the $M \times 1$ complex-valued vector in frequency space of acoustic pressures recorded by M microphones in the array. $\mathbf{g}(\mathbf{x_t})$ is the propogation Green's function relating $\mathbf{P}(\omega)$ to a theoretical source of strength q at position $\mathbf{x_t}$, as in Equation 2. The superscript 'H' refers to the Hermitian transpose.

$$B(\mathbf{x_t}, \omega) = \frac{\mathbf{g}(\mathbf{x_t}, \omega)^H \overline{\mathbf{P}(\omega)\mathbf{P}(\omega)^H} \mathbf{g}(\mathbf{x_t}, \omega)}{|\mathbf{g}(\mathbf{x_t}, \omega)|^4} \tag{1}$$

$$\mathbf{P}(\omega) = \mathbf{g}(\mathbf{x_t}, \omega) q(\mathbf{x_t}) \tag{2}$$

In Equation 1, $\overline{\mathbf{P}(\omega)\mathbf{P}(\omega)^H}$ is known as the cross spectral matrix (CSM) and denoted $\mathbf{G}$. The overbar denotes the averaging over the Fourier transforms in a number of discrete time blocks. $\mathbf{g}(.)$ is chosen based on the experimental conditions and the type of source to be investigated.

Liu et al. (2008) showed that for a dipole source with spatial orientation $\vec{\zeta}$ in an open jet test facility, the propogation Green's function is given by Equation 3, where $r_s(\mathbf{x_t}, \mathbf{x_i})$ denotes the distance travelled by individual ray paths from the point $\mathbf{x_t}$ to the i^{th} microphone location $\mathbf{x_i}$ through the shear layer of the open jet. $c_i(\mathbf{x})$ is a term that accounts for the amplitude attenuation of the ray from the point $\mathbf{x_t}$ to $\mathbf{x_i}$ because of shear layer interaction.

$$g_i(\mathbf{x}) = c_i(\mathbf{x}) \frac{e^{-jkr_s(\mathbf{x_t}, \mathbf{x_i})}}{4\pi r_s(\mathbf{x_t}, \mathbf{x_i})} \vec{\zeta} \cdot \frac{\mathbf{x} - \mathbf{x_i}}{|\mathbf{x} - \mathbf{x_i}|} \tag{3}$$

2.2 Multiplicative Beamforming

In this paper, 'multiplicative beamforming' is used as an alternative beamforming processing technique specific to three-dimensional beamforming using a non-planar array of microphones. Essentially conventional planar beamforming is performed on a 3D scanning grid for two different portions of the microphone array. The results are then piecewise multiplied together to obtain the final solution.

In principle, multiplicative beamforming may be peformed on any number of sets of microphones in any orientation. For this paper, the technique performed on two mutually perpendicular sets of microphones, each with an equal number of microphones. Let the subscript 1 denote the first array and the subscript 2 denote the second array. Then following conventional beamforming analysis, the output of each array is:

$$B_{t1} = \frac{\mathbf{g_1}(\mathbf{x_t})^{\mathbf{H}} \mathbf{G_1} \mathbf{g_1}(\mathbf{x_t})}{|\mathbf{g_1}(\mathbf{x_t})|^4} \tag{4}$$

$$B_{t2} = \frac{\mathbf{g_2}(\mathbf{x_t})^{\mathbf{H}} \mathbf{G_2} \mathbf{g_2}(\mathbf{x_t})}{|\mathbf{g_2}(\mathbf{x_t})|^4} \tag{5}$$

where $\mathbf{G_1}$ and $\mathbf{G_2}$ denote the cross-spectral matrices for microphone set 1 and 2, and $\mathbf{g_1}$ and $\mathbf{g_2}$ denote the Green's functions associated with each microphone set. The final result at grid point $\mathbf{x_t}$ is the square root of the product of the two;

$$B_t = \sqrt{B_{t1} B_{t2}} \tag{6}$$

The square root ensures that B_t will yield the true source power when the beamformer is steered to the true source position, $\mathbf{x_s}$, i.e when $\mathbf{x_t} = \mathbf{x_s}$.

If the output for each positon, B, is represented in vector form, $\mathbf{b}$, then the final output is the square root of the Hadamard (element wise) product of the two vectors;

$$\mathbf{b} = \sqrt{\mathbf{b_1} \circ \mathbf{b_2}} \tag{7}$$

The above formulation requires the calculation of two CSMs corresponding to the two different sets of microphones. Alternatively, a single cross-spectral matrix, $\mathbf{G}$, using all the microphones in the array can be used if appropiate weighting matrices, $\mathbf{W_1}$ and $\mathbf{W_2}$, are chosen and utilised in Equations 4 and 5 as follows:

$$B_{t1} = \frac{\mathbf{g}(\mathbf{x_t})^{\mathbf{H}}\mathbf{W_1}\mathbf{G}\mathbf{W_1}\mathbf{g}(\mathbf{x_t})}{|\mathbf{W_1}\mathbf{g}(\mathbf{x_t})|^4} \tag{8}$$

$$B_{t2} = \frac{\mathbf{g}(\mathbf{x_t})\mathbf{W_2}\mathbf{G}\mathbf{W_2}\mathbf{g}(\mathbf{x_t})}{|\mathbf{W_2}\mathbf{g}(\mathbf{x_t})|^4} \tag{9}$$

where $\mathbf{g}(\mathbf{x_t})$ is now the Green's function which encompases propogation of sound from $\mathbf{x_t}$ to all microphones in the array. Each element of the weight matrix, W_{ii} where $i = 1, ..., M$, is defined as follows;

$$W_{ii} = \begin{cases} 1 & i \in \text{microphone set} \\ 0 & i \notin \text{microphone set} \end{cases} \tag{10}$$

3. NUMERICAL SIMULATION OF A DIPOLE SOURCE USING CONVENTIONAL AND MULTPLICATIVE BEAMFORMING

To compare conventional and multiplicative beamforming, a numerical (synthetic) cross-spectral matrix was generated for a dipole source and analysed using a synthetic microphone array. For a dipole source with orientation $\vec{\zeta}$, the root mean square pressure at a distance, $r = |\mathbf{x_s} - \mathbf{x_i}|$ from the source in the far-field with no flow can be expressed as,

$$p_{rms}(r) = C \times \left\{ \vec{\zeta} \cdot \frac{\mathbf{x_s} - \mathbf{x_i}}{r} \right\} \tag{11}$$

where C is constant and the term in the braces governs the directionality of the source. With the known positions of the microphones in the synthetic microphone array, the pressure records at each microphone, $\mathbf{P_{synth}}$, can be calculated from Equation 11. A synthetic CSM can then be generated by

$$G_{synth} = \overline{\mathbf{P_{synth}}\mathbf{P_{synth}}^H} \tag{12}$$

3.1 Numerical 3D Beamforming of a Dipole Source.

Figure 1 shows the response of a planar array measuring a (synthetically generated) dipole source at 3000 Hz using conventional beamforming. The array is comprised of 31 pressure receivers arranged in an Underbrink spiral pattern with an outer diameter of 0.5 m. The plane of the array is given by $z = 0.5$. In this case, the dipole source is is located at $\mathbf{x_s} = (0,0,0)$. In the simulations the constant C was chosen so that source power was 100 dB/Hz re. $20\mu pa.s^{-1}$. The response is shown as isocontours of levels up to 3 dB down from the maximum source power. The result shows that the beamwidth of the array is narrow (high resolution) for directions parallel to the array but highly elongated (low resolution) for directions perpendicular to the array. This demonstrates the poor depth resolution of planar arrays.

Figure 2 shows the results obtained with conventional beamforming using two arrays to partially enclosing the source. The second array has the same pattern as the first, but it located in the plane $y = 0.5$. The spatial resolution is improved, but the isocontour is elongated, this time in the direction of the array centre, which is the intersection of the two array planes. A side lobe is also introduced below the location of the dipole. This is due to the properties of the dipole Green's function used. More details are outlined in Liu et al. (2008).

Finally, Figure 3 shows the source map obtained using multiplicative beamforming. The multiplicative processing retains the good spatial resolution from each mutually orthogonal planar array and multiplies out the poor spatial resolution normal to each of the arrays. The result is no directional bias in the isocontour. The side lobe remains but is significantly reduced in amplitude.

4. EXPERIMENTAL ANALYSIS

Multiplicative beamforming was then applied to aeroacoustic data taken in an open-jet anechoic wind tunnel at the University of Adelaide. The facility is the same used by Moreau et al. (2013). The beamformer inside the facility was similar in arrangement to the one used in the simulations. The microphone array consists of 62 G.R.A.S 40PH phase matched microphones arranged in two Underbrink spiral pattern subarrays of 31 microphones each. An Underbrink pattern was chosen because it has superior performance over other spiral array designs (Prime and Doolan 2013) such as the B&K spiral design, multi-spiral design, Dougherty spiral design and Archimedian spiral design. The microphones are press fit into 12 mm MDF sheet with an EchoSorb 25 sound absorption layer covering the top. Each microphone head is covered with a wind sock to isolate it from low level recirculation inside the wind tunnel chamber. One subarray is located 0.5 m above the midplane

of the exit nozzle and the other subarray is located 0.5 m laterally from the midplane of the exit nozzle. The centre microphone of each spiral is located 360 mm downstream of the exit plane. A schematic and photograph of the experimental set up is shown in Figures 4 and 5.

The beamforming measurements were performed for the test model of a cylinder in uniform flow at 32 m/s. The cylinder had a diameter of 4 mm and the axis of the cylinder was located 110 mm downstream of the nozzle exit plane. The length of the cylinder was 400 mm, so that it exceeded the width of the nozzle, essentially making it a semi-infinite cylinder. The cylinder was mounted in such a way to eliminate boundary layer interaction at the mounting points. A picture of the cylinder mounting arrangement is shown in Figure 6.

4.1 Experimental 3D Beamforming of a Dipole Source.

Figures 7 through 10 show the experimentally obtained beamforming results of the semi-infinite cylinder using both conventional beamforming and multiplicative beamforming. The results are shown in energy bandwidths of 100 Hz at centre frequencies of 1600 Hz and 4800 Hz. At these frequencies a strong dipole orientated perpendicular to the flow (in the z-direction) is expected due to vortex shedding.

The results using conventional beamforming show an elongated lobe that generally falls on the cylinder midspan. The size of the lobe at 4800 Hz is considerably smaller than that at 1600 Hz. This is due to the improved resolution of the beamformer at higher frequencies.

The sound maps obtained with multiplicative beamforming generally improve the quality of the source localisation because the lobes are no longer elongated. They are instead spherical and centered on the midpsan of the cylinder. Again the lobe at 4800 Hz is smaller than that at 1600 Hz because of the improved resolution at shorter wavelengths. Small side lobes are apparent below the main lobe that are due to the properties of the dipole Green's function used in the analysis.

5. CONCLUSIONS

Multiplicative beamforming has been demonstrated as a suitable alternative processing technique for 3D acoustic source localisation using a non-orthogonal array of microphones where the source is not fully enclosed by the array. Numerical simulations show that multiplicative beamforming eliminates the directional bias in the main lobe present in conventional beamforming. The method was also tested experimentally on a dipole source of radiation in an anechoic wind tunnel. The experimental results show that multplicative beamforming provides improved spatial resolution and source localisation of the dipole sound source.

6. ACKNOWLEDGEMENTS

The visit of Vincent Valeau to the University of Adelaide was sponsored by Région Poitou-Charentes.

REFERENCES

Bies, D. A. and C. H. Hansen (2009). *Engineering Noise Control; Theory and Practice*. CRC Press.

Brooks, T. F. and W. M. Humphreys (1999). "Effect of directional array size on the measurement of airframe noise components". In: *5th AIAA/CEAS Aeroacoustic conference, AIAA Paper 99-1958* (cit. on p. 1).

— (2003). "Flap-edge aeroacoustic measurements and predictions". In: *Journal of Sound and Vibration* 261, pp. 31–74 (cit. on p. 1).

Geyer, T., E. Sarradji, and J. Giesler (2012). "Application of a beamforming technique to the measurement of airfoil leading edge noise". In: *Advances in Acoustics and Vibration*. DOI: 10.1155/2012/905461 (cit. on p. 1).

Liu, Y., A. R. Quayle, A. P. Dowling, and P. Sijtsma (2008). "Beamforming correction for dipole measurement using two-dimensional microphone arrays". In: *Acoustical Society of America* 124 (1), pp. 182–191. DOI: 10.112/1.2931950 (cit. on pp. 1–3).

Moreau, D. J., Z. Prime, R. Porteous, C. J. Doolan, and V. Valeau (2013). "Flow-induced noise of a wall-mounted finite airfoil atlow-to-moderate Reynolds number". In: *Journal of Sound and Vibration* (cit. on p. 3).

Padois, T., Robin, and A. Berry (2013). "3D source localisation in a closed wind-tunnel using microphone arrays". In: *19th AIAA/CEAS Aeroacoustics Conference, Berlin, Germany* (cit. on p. 1).

Prime, Z. and C. J. Doolan (2013). "A comparison of popular beamforming arrays". In: *Proceedings of Acoustics 2013 - Victor Harbor* (cit. on pp. 1, 3).

Sarradj, E. (2012). "Three-dimensional acoustic source mapping with different beamforming steering vector formulations". In: *Advances in Acoustics and Vibration*. DOI: 10.1155/2012/292695 (cit. on p. 1).

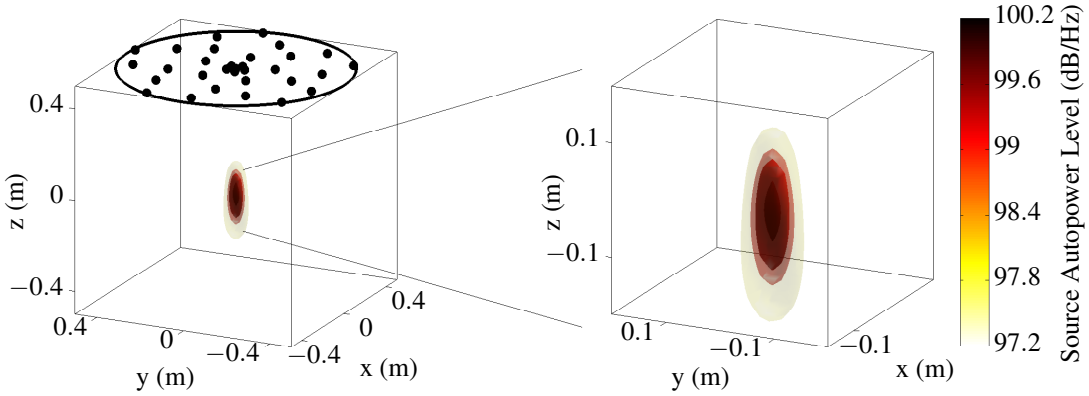

Figure 1 – Beamforming source map of a synthetically generated dipole source with no mean flow using one planar array. The elongated isocontour demonstrates the poor depth resolution of a planar array of microphones.

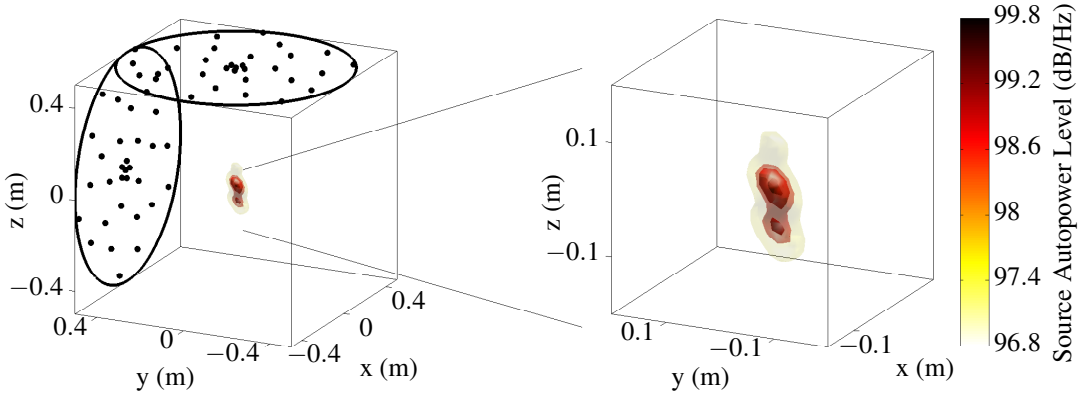

Figure 2 – Beamforming source map of a synthetically generated dipole source with no mean flow using two perpendicular planar arrays. Although the resolution is enhanced, the elongated isocontour toward the array centre demonstrates the directional bias inherent in conventional beamforming.

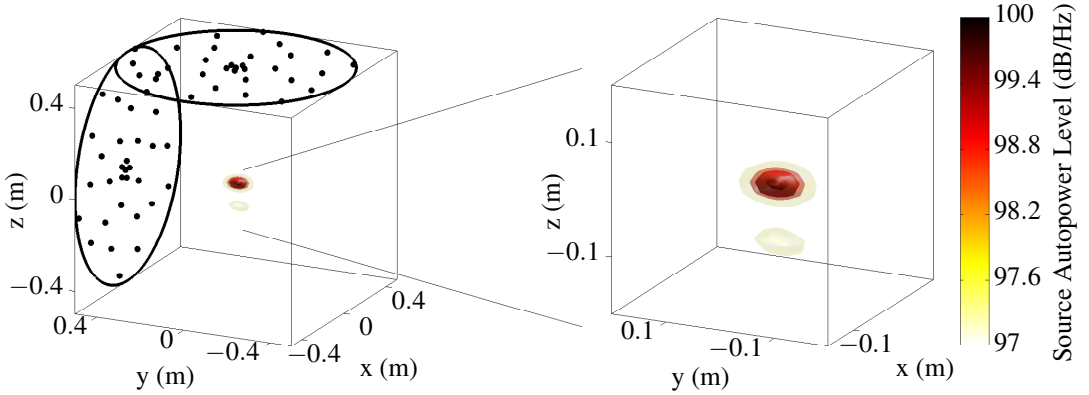

Figure 3 – Multiplicative beamforming source map synthetically generated dipole source with no mean flow using two perpendicular planar arrays. The homogenous source map demonstrates the utility of multiplicative beamforming.

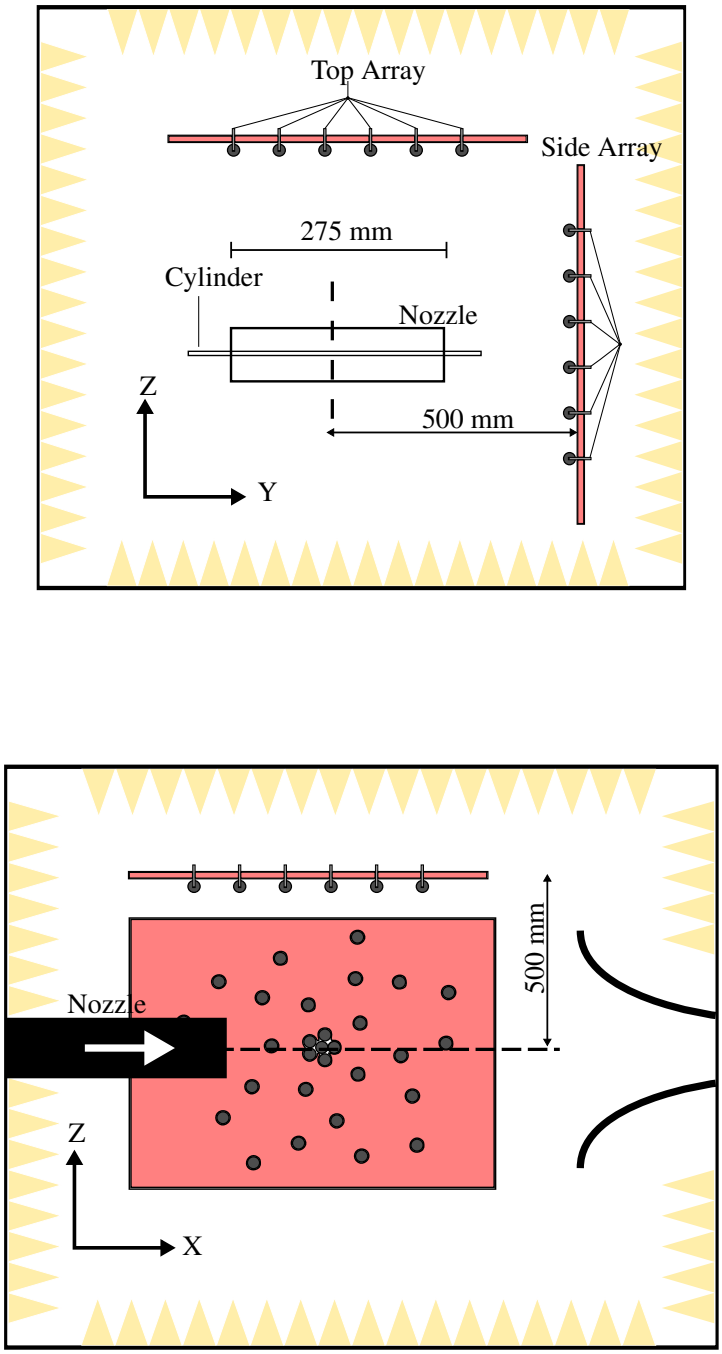

Figure 4 – Schematic of the 62 channel dual spiral microphone array inside the AWT. The array is comprised of two perpendicular subarrays each arranged in an Underbrink spiral around the open-jet nozzle. The top figure is an end view with the flow coming out of the page while the bottom figure is a side view with the flow going from left to right.

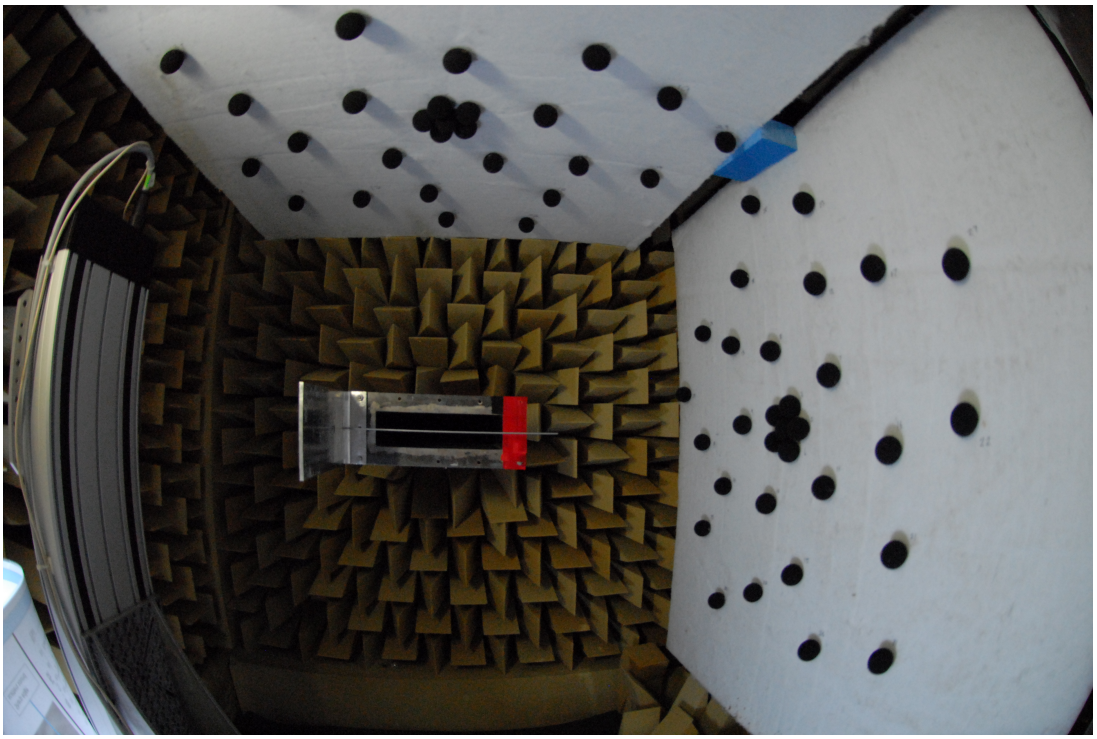

Figure 5 – Photograph of the experimental setup inside the AWT, taken downstream of the nozzle exit.

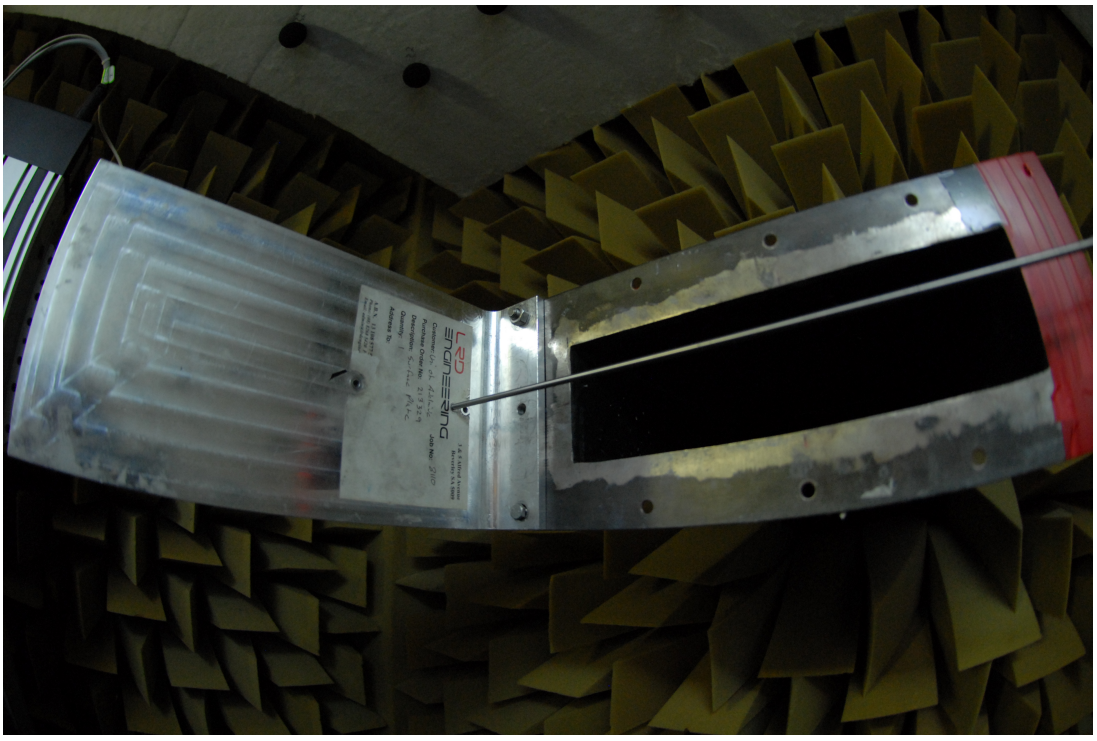

Figure 6 – Photograph of the cylinder mounting setup. The cylinder is mounted so that no boundary layer is developed at the cylinder mounting point.

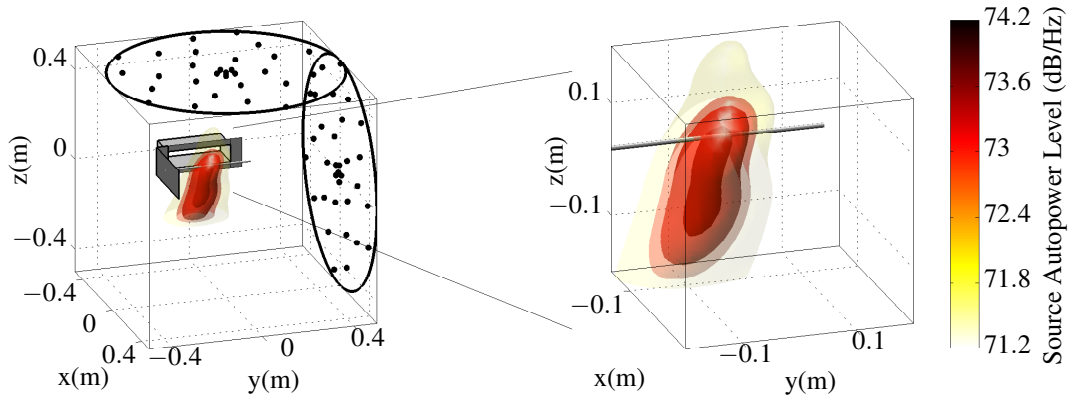

Figure 7 – Beamforming source map of an experimentally obtained dipole source using conventional beamforming at 1600 Hz.

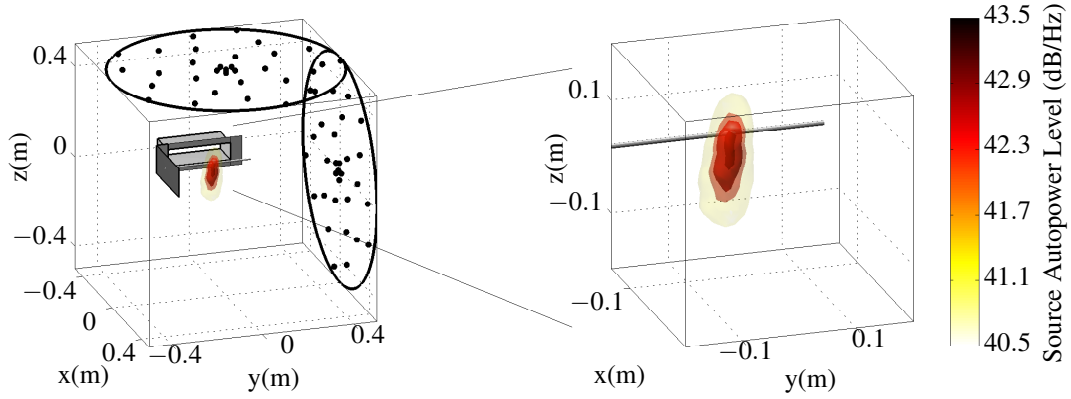

Figure 8 – Beamforming source map of an experimentally obtained dipole source using conventional beamforming at 4800 Hz.

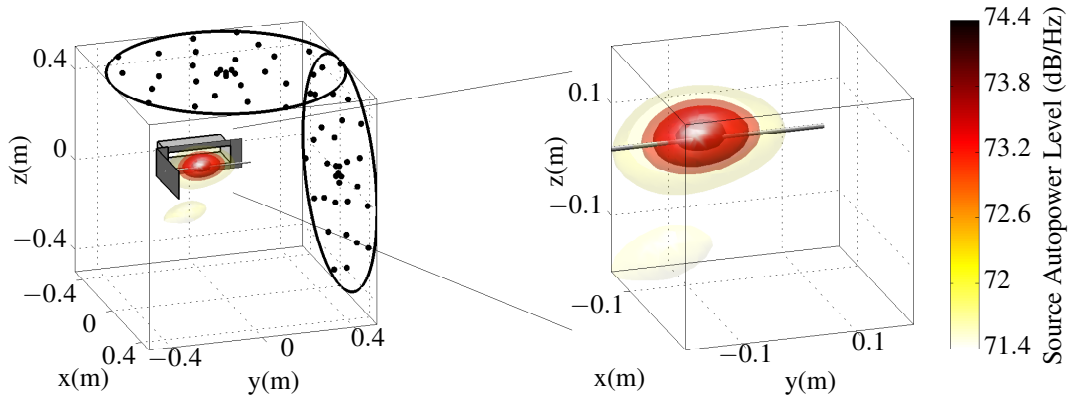

Figure 9 – Beamforming source map of an experimentally obtained dipole source using multiplicative beamforming at 1600 Hz.

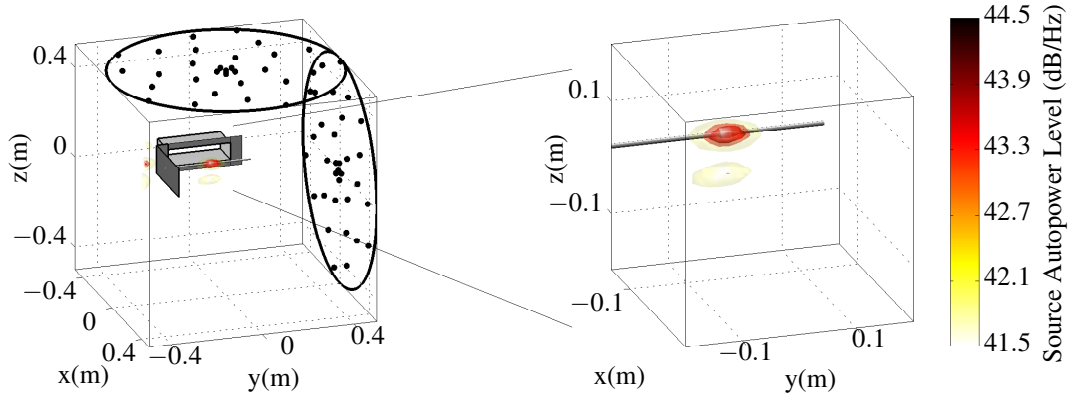

Figure 10 – Beamforming source map of an experimentally obtained dipole source using multiplicative beamforming at 4800 Hz.